Development of hyaluronan-based dissolving microneedle arrays for dermal vaccination

Leone, M.

Chapter 5

Hyaluronan molecular weight: effects on dissolution time of dissolving microneedles in the skin and on immunogenicity of antigen

Adapted from Eur J Pharm Sci 2020 (146): 105269

Mara Leone[1], Stefan Romeijn[1], Bram Slütter[1], Conor O'Mahony[2], Gideon Kersten[1,3,*], Joke A. Bouwstra[1,*]

[1] Division of BioTherapeutics, Leiden Academic Centre for Drug Research (LACDR), Leiden University, Leiden, the Netherlands

[2] Tyndall National Institute, University College Cork, Cork, Ireland

[3] Institute for Translational Vaccinology (Intravacc), Bilthoven, the Netherlands

[*] These authors contributed equally.

ABSTRACT

Biomaterials used as matrix for dissolving micro needles (dMNs) may affect the manufacturing process as well as the potency of the active pharmaceutical ingredient, e.g. the immunogenicity of incorporated vaccine antigens. The aim of this study was to investigate the effect of the molecular weight of hyaluronan, a polymer widely used in the fabrication of dMNs, ranging in molecular weight from 4.8 kDa to 1.8 MDa, on the dissolution of microneedles in the skin in time as well as the antibody response in mice and T-cell activation *in vitro*. Hyaluronan molecular weight (HA-MWs) did not affect antibody responses (when lower than 150 kDa) nor CD4+ T-cell responses against model antigen ovalbumin. However, the HA-MWs had an effect on the fabrication of dMNs. The 1.8 MDa HA was not suitable for the fabrication of dMNs. Similarly, the 4.8 kDa HA generated dMN arrays less robust compared to the other HA-MWs requiring optimization of the drying conditions. Finally, higher HA-MWs led to longer application time of dMN arrays for a complete dissolution of microneedles into the skin. Specifically, we identified 20 kDa HA as the optimal HA-MW for the fabrication of dMNs as with this MW the dMNs are robust and dissolve fast in the skin without affecting immunogenicity.

GRAPHICAL ABSTRACT

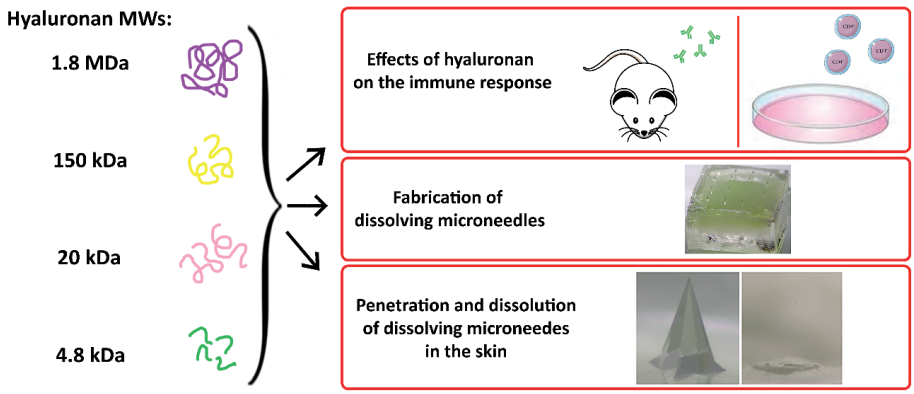

Keywords: dissolving microneedles, hyaluronan, molecular weight, immune response, dermal vaccine delivery.

1. INTRODUCTION

Microneedles are intensively studied for dermal and transdermal drug and vaccine delivery [1, 2]. Microneedles are needle-like structures up to 1 mm in length, capable of piercing the upper layer of the skin, the *stratum corneum*, enabling drug and vaccine delivery in a minimally invasive and painless way [3, 4]. Several microneedle concept are in development: i) hollow microneedles to inject liquid formulations through the bore of the microneedle, ii) microneedles for skin pretreatment to create microchannels prior application of a patch containing the drug or vaccine formulation, iii) porous, coated, hydrogel-forming microneedles and dissolving microneedles that release the drug or vaccine upon insertion into the skin [5-8]. Dissolving microneedles (dMNs), completely dissolve after insertion into the skin, thereby releasing the encapsulated drug or vaccine [3]. As an additional advantage, the dry state of dMNs combined with the presence of excipients can increase protein thermostability [3].

dMNs are produced from different materials, ranging from low molecular weight carbohydrates to biodegradable polymers [3]. The selection of the matrix material is based on different factors such as i) safety, ii) compatibility with the active compound and the manufacturing procedure, iii) capability of the manufactured dMNs to efficiently pierce the skin and subsequently dissolve in a short time period and iv) potential adjuvant properties. One of the most frequently used matrix material is the hyaluronan (HA) [3, 9-13]. High molecular weight HA is a non-toxic, biodegradable, biocompatible and non-inflammatory linear polysaccharide [14] naturally present in the skin and approved by the FDA as inactive material.

Although frequently used for microneedle manufacturing, the molecular weight of the polysaccharide HA is rarely addressed [1, 3, 9, 11, 12, 15-17]. There are indications however, that the molecular weight of the HA influences its immuno-adjuvant properties. Only high molecular weight HA (HMW-HA, MW 10^7 Da) is an ubiquitous extracellular matrix component [18, 19]. Low molecular weight HA (LMW-HA) (4- to 16-oligosaccharide size, 800 – 3200 Da [19, 20]) is able to activate immunocompetent cells such as macrophages [21] and DCs [19-23]. These activated human DCs are able to stimulate T-cell mediated immune responses [19, 20, 24]. The immune activation is mediated by the HA binding to specific receptors such as CD44, CD168, Toll-like receptor (TLR)-2 and TLR-4 [25-28]. The latter is a receptor associated with the innate immunity and the host defence against bacterial infection [20]. In the presence of antigens, a specific response may develop [29] and so the LMW-HA can act as an adjuvant during vaccination.

In a previous study from our group, the dissolving microneedle properties of the only 150 kDa HA, such as penetration and dissolution in the skin, have been reported [30].

The aim of this study was to determine whether i) HA with different MW had an effect on the immune response for both antibody (*in vivo* injections by hMN) and cellular (*in vitro* T-

cell exposure) responses and ii) it was possible to fabricate dMNs by micromolding from HA with different molecular weight. To this end, first the potential adjuvant effect of HA was assessed by i) performing immunization studies investigating the antibody response in mice injected with the model antigen ovalbumin (OVA) in presence of a range of different HA-MWs and ii) investigating T-cell activation *in vitro* upon exposure to several HA-MWs with OVA. Subsequently, different HA-MWs were used to fabricate dMNs assessing the compatibility of the matrix material of each MW with the manufacturing procedure. These dMNs were used to investigate their capability to pierce the skin and to dissolve in reasonable short time period.

2. MATERIALS AND METHODS

2.1 Materials

Hyaluronan (HA) (sodium hyaluronate, average Mw was 4.8 kDa, 20 kDa and 150 kDa (endotoxin level ≤ 0.05 EU/mg) or 1.8 MDa (endotoxin level ≤ 0.07 EU/mg)) was purchased from Lifecore Biomedical (Chaska, MN, USA). Immunization studies, ELISA and cell culturing were performed by using endotoxin-free ovalbumin (OVA) (endotoxin level < 1 EU/mg) from Invivogen (Toulouse, France). PBS pH 7.4 for hMN injections was obtained from B. Braun, Melsungen, Germany.

For cell culture, Ca^{2+}- and Mg^{2+}-free phosphate-buffered saline (PBS), Iscove's Modified Dulbecco's Medium (IMDM), Roswell Park Memorial Institute Medium (RPMI 1640), penicillin/streptomycin and l-glutamine were purchased from Lonza (Basel, Switzerland). Fetal calf serum (FCS) and granulocyte-macrophage colony-stimulating factor (GM-CSF) were purchased from GE Healthcare (Little Chalfont, UK) and PeptroTech (London, UK) respectively. Lipopolysaccharide (LPS) extracted from Salmonella typhosa, CFSE and β-mercaptoethanol were purchased from Sigma-Aldrich (Zwijndrecht, the Netherlands).

The antibodies CD25-APC (PC 61.5), CD69-PE (H1.2F3), Thy1.2-PE-Cy7 (53–2.1), CD4-eFluor450 (GK1.5), Vα2 TCR-PE (B20.1) and fixable viability dye-eFluor780 were purchased from eBioscience (Thermofisher Scientific, MA, USA).

For dissolving microneedle fabrication, 10 mM PB (7.7 mM Na_2HPO_4, 2.3 mM NaH_2PO_4, pH 7.4) was prepared in the laboratory. Vinylpolysiloxanes A-silicone (Elite Double 32a Normal) and the two-component epoxy glue (Bison, Goes, The Netherlands) were obtained from The Zhermack Group (Badia Polesine, Italy) and Bison International B.V. (Goes, The Netherlands), respectively. Polydimethylsiloxane (PDMS, Sylgard 184) was purchased from Dow Corning (Midland, MI, USA). Solid silicon MNs, obtained through a potassium hydroxide wet-etching process [31], were kindly provided by the Tyndall National Institute (Cork, Ireland). All the chemicals were of analytical grade and Milli-Q water (18 MΩ/cm, Millipore Co.) was used for the preparation of all solutions.

2.2 Animals

Immunization studies were performed using female BALB/c (H2d), 8-11 weeks old (Charles River, Maastricht, The Netherlands) and randomly assigned to groups of 8. The studies were approved by the ethical committee on animal experiments of Leiden University (License number (14176).

For *in vitro* T-cell activation studies, C57BL/6 and OT-II transgenic mice on a C57BL/6 background were purchased from Jackson Laboratory (CA, USA), bred in-house under standard laboratory conditions, and provided with food and water ad libitum. All animal work was performed in compliance with the Dutch government guidelines and the Directive 2010/63/EU of the European Parliament. Experiments were approved by the Ethics Committee for Animal Experiments of Leiden University (CCD number AVD106002017887).

2.3 Hollow microneedles

Hollow microneedles (hMNs) were prepared as described previously [32, 33] (a representative image of a hMN is reported in the Supplementary data, Figure S1). Briefly, polyimide-coated fused silica capillaries (Polymicro, Phoenix AZ, 375 µm outer diameter, 50 µm inner diameter) were filled with silicone oil in a vacuum oven (100 ° C) overnight. Subsequently, the capillaries were etched during 4 h in ≥ 48% hydrofluoric acid and the polyimide coating was removed from the ends of the capillaries by diving them into heated (250 °C) sulfuric acid for 5 min.

2.4 Immunization studies

BALB/c mice were anesthetized by intraperitoneal injection of 150 mg/kg ketamine and 10 mg/kg xylazine and the injection site was shaved (flank, approximately 4 cm^2). The same day, mice were immunized by intradermal hMN injection (120 µm injection depth) of 10 µl with 0.31 µg OVA with 3.1 µg HA for each HA-MW dissolved in PBS pH 7.4. Intradermal hMN injection of each HA-MWs without OVA and PBS were included as control. For controlled depth intradermal microinjections, a hollow-microneedle applicator was used as reported previously [32].

Immunizations were performed at day 1 (prime), day 22 (boost) and day 43 (2nd boost). Prior to each immunization, a blood sample was collected from the tail vein. At day 63, the blood sample was collected from the femoral artery and all mice were sacrificed. Serum was isolated from the samples and stored at - 80°C.

2.5 Determination of OVA-specific IgG antibodies

OVA-specific antibodies were analysed by a sandwich enzyme-linked immunosorbent assay (ELISA) as described earlier [10]. Briefly, well-plates were coated with OVA for 1.5 h at 37 °C and then blocked with bovine serum albumin (BSA) (Sigma-Aldrich, Zwijndrecht, the Netherlands). After the blocking, three-fold serial dilutions of serum were applied to the plates and incubated for 1.5 h at 37 °C. Then, the plates were incubated with horseradish peroxidase-conjugated goat antibodies against IgG total, IgG1 and IgG2a (Southern Biotech, Birmingham, AL, USA) for 1 h at 37 °C. Finally, 1-step TM ultra 3,3′,5,5′-tetramethylbenzidine (TMB) (Thermo-Fischer Scientific, Waltham, USA) was used as substrate and sulfuric acid (H_2SO_4) (95–98%) (JT Baker, Deventer, The Netherlands) was added to stop the reaction. The absorbance was measured at 450 nm on a Tecan Infinite M1000 plate reader (Männedorf, Switzerland) and the antibody titers were determined as the log10 value of the mid-point dilution of a complete s-shaped absorbance-log dilution curve of the diluted serum level.

2.6 Bone marrow-derived dendritic cells (BMDCs)

To examine T-cell activation *in vitro*, first bone marrow was isolated from the tibias and femurs of C57BL/6 female mouse. A single-cell suspension of bone marrow cells was obtained by using a 70 µm cell strainer (Greiner Bio-One B.V., Alphen aan den Rijn, NL). The cells were cultured in IMDM medium supplemented with 2 mM l-glutamine, 8% (v/v) FCS, 100 U/ml penicillin/streptomycin and 50 µM β-mercaptoethanol at 37 °C and 5% CO_2 in 95 mm Petri dishes (Greiner Bio-One B.V., Alphen aan den Rijn, NL) and 20 ng/ml GM-CSF for 10 days. Medium was refreshed every other day.

On day 11, the BMDCs were harvested from the petri dish and distributed into 96-well plates (100 µl/well, 10 000 cells/well). Then, 100 µl/well of formulations consisting of: i) 5 µg OVA, ii) 5 µg OVA mixed with 50 µg HA (per each molecular weight) or iii) 50 µg HA (per each molecular weight) were added to the wells. OVA (5 µg/well) + LPS (100 ng/well) or LPS (100 ng/well) were added as positive control; medium was included as negative control.

The BMDCs were exposed to the formulations overnight at 37 °C and 5% CO_2 and subsequently OVA-specific $CD4^+$ T-cells were transferred on BMDCs in co-culture experiments (see 2.6).

2.7 $CD4^+$ T-cell activation by antigen loaded BMDC

OT-II (OVA-specific $CD4^+$) T-cells were obtained from the spleen of OT-II transgenic C57BL/6 mouse. Single cell suspensions were obtained by forcing the spleens through a 70 µm strainer. After erythrocyte depletion with lysis-buffer (0.15 M NH_4Cl, 1 mM $KHCO_3$, 0.1 mM

Na_2EDTA; pH 7.3), staining with CFSE was performed. Briefly, cells were suspended in PBS containing 1 µM CFSE and incubate 10 min at room temperature. CFSE was neutralized by FCS addition and the cells were washed with RPMI to remove excess of CFSE.

At this point, the percentage of $CD4^+/Valpha^{2+}$ cells was determined by flow cytometry (BD FACSCanto-II, San Jose, CA). OT-II cells were transferred on BMDCs previously exposed to the formulations (50 000 cells/well).

On day 15, the cell surfaces were stained by incubating the cells with fixable viability dye-eFluor780 (1:1000) and fluorescently labelled antibodies specific for: Thy1.2-PE-Cy7 (1:500), CD25-APC (1:500), CD69-PE (1:500) and CD4-eFluor450 (1:500) for 30 min (100 µl/well) at 4 °C. After 30 min, the excess antibodies were washed by using FACS buffer. The cells were incubated with fixation and permeabilization solution (BD Biosciences) for 10 min at 4 °C. Finally, the cells were washed with FACS buffer and analysed by flow cytometry (BD FACSCanto-II, San Jose, CA). The data were analysed by using FlowJo software.

2.8 Fabrication of dissolving microneedles

dMN arrays were prepared as described previously [10]. HA 10% (w/v) was dissolved in phosphate buffer (10 mM, pH 7.4) and stored overnight. The next day, HA solution was poured in each well of the polydimethylsiloxane mold (PDMS, Sylgard 184, Dow Corning, Midland, MI, USA) to prepare dMN arrays (4 by 4 dMNs per array of 300 µm length and 100 µm base diameter). After several steps of vacuum and centrifuge, the 20 kDa and 150 kDa HA arrays were oven-dried overnight at 37°C. As this procedure result in fragile dMN arrays when using 4.8 kDa HA, these dMN arrays were dried at room temperature overnight. The next day, a backplate was produced by pouring a mixture of vinylpolysiloxane base and catalyst (in a 1:1 ratio) (Elite Double 32a Normal, Zhermack Group, Badia Polesine, Italy) and subsequently a two-component glue solution (Bison International B.V., Goes, The Netherlands) onto each array and left curing.

Finally, the arrays were removed from the PDMS mold and inspected for shape and sharpness by light microscopy (Stemi 2000-C, Carl Zeiss Microscopy GmbH, Göttingen, Germany).

2.9 Human skin

Human abdomen skin was obtained from a local hospital within 24 hours after cosmetic surgery according to the declaration of Helsinki. The fat excess was removed with a scalpel and the skin was stored at -80°C. Before use, the skin was thawed at 37°C for 1 h in a humid petri dish and stretched with pins on parafilm-covered styrofoam. Before starting the experiment, the skin was cleaned with Milli-Q and 70% ethanol.

2.10 Penetration of microneedles in *ex vivo* human skin

dMN arrays (n=3 per HA-MW) were applied onto the skin by impact velocity, as described elsewhere [10, 34], by using an impact insertion applicator with a constant velocity of 0.54 m/s (Leiden University - applicator with uPRAX controller version 0.3). The dMNs were kept in the skin for 18 seconds and withdrawn. Then, the pierced skin was treated with trypan blue, as previously described [35] and *stratum corneum* was removed by tape stripping. Finally, the blue spots were visualized using a light microscope (Axioskop and Stemi 2000-C, Carl Zeiss Microscopy GmbH, Göttingen, Germany) (a representative image of pierced skin is reported in the Supplementary data, Figure S2) and the penetration efficiency per array was calculated by dividing the number of blue spots by the number of dMNs on the array (16) (Equation 1).

$$\text{Penetration efficiency} = (\text{number of blue spots})/16 \times 100 \qquad \text{(Eqn. 1)}$$

2.11 Dissolution of microneedles in *ex vivo* human skin

A dMN array (n=7) was applied on the skin as described in section 2.10 and was kept in the skin for 1 min, 5 min, 10 min or 20 min. The microneedle length before and after dissolution was determined with a light microscope (Axioskop and Stemi 2000-C, Carl Zeiss Microscopy GmbH, Göttingen, Germany) equipped with a digital camera (Axiocam ICc 5, Carl Zeiss). In order to obtain the dMN dissolved volume for each insertion period, dissolved microneedle length was measured by ZEN 2012 blue edition software (Carl Zeiss Microscopy GmbH) and the dissolved MN volumes were calculated as reported in our previous study in supplementary Figure 3 [10].

2.12 Statistics

IgG titers and T-cell response were analysed using one-way ANOVA with respectively Bonferroni and Tukey's post-test suitable in the software Prism (Graphpad, San Diego, USA). A p-value less than 0.05 was considered to be significant.

Microneedle penetration efficiency was analysed by Kruskal-Wallis test with Dunn's multiple comparison test ($p < 0.05$).

The remaining dMN length after dissolution at different time points was analysed by two-way ANOVA with a Tukey's post-test ($p < 0.05$).

3. RESULTS

3.1 Immunization studies

The liquid formulations of OVA alone or mixed with different HA-MWs was intradermally injected by using hollow microneedles. During injection no problems with clogging or leakage were observed. The formation of a blister on the site of the injection indicated a successful intradermal delivery of the formulation. No adverse effects were observed.

The OVA-specific total IgG titers increased after each immunization (Figure 1A-C). The presence of HA, regardless of the molecular weight, did not increase the total IgG response compared to the injection of OVA only. After the first boost, a higher OVA specific IgG response in the mice immunized with OVA-HA 4.8 kDa was observed compared to the mice injected with OVA-HA 150 kDa ($p<0.01$). However, both OVA-HA 4.8 kDa and OVA-HA 1.8 MDa resulted in equal responses compared to the OVA only group. After the second boost, the group immunized with OVA-HA 1.8 MDa showed lower OVA-specific total IgG titers than OVA only and OVA-HA 4.8 kDa, suggesting a detrimental effect on adding high molecular weight HA. Overall, the presence of high MW HA seemed to reduce the immunogenicity of the antigen while the presence of HA regardless of the molecular weight did not enhance the immune response compared with OVA alone.

The IgG1 response (Figure 1 D-F) followed the same trend as the total IgG response: the presence of HA in different molecular weights did not change the response compared to OVA alone after each immunization. Intradermal injection of OVA, with or without HA, resulted in undetectable OVA specific IgG2a responses (data not shown).

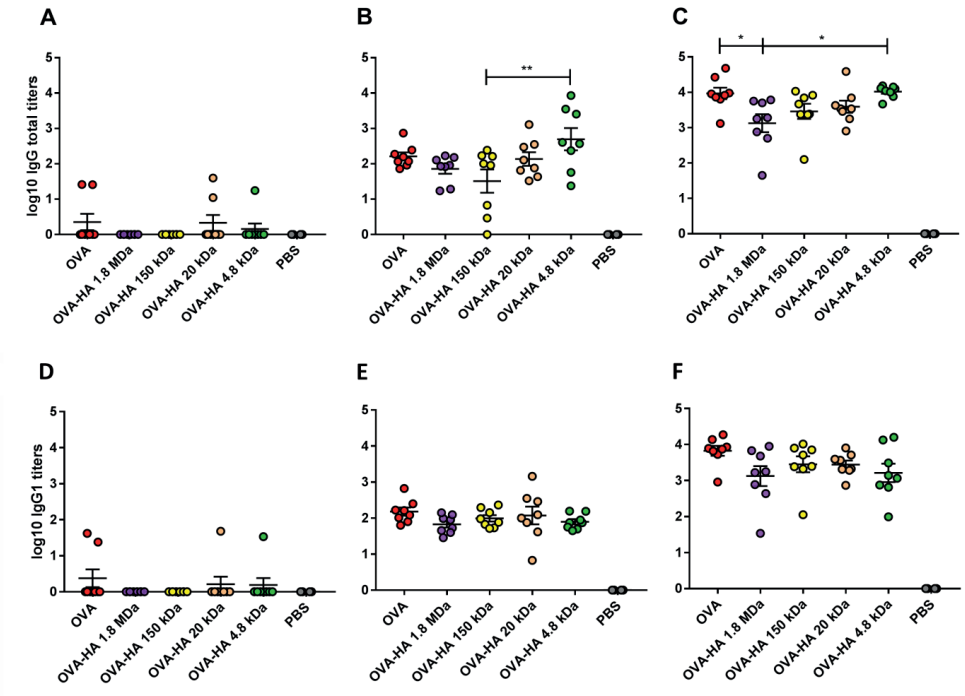

Figure 1. OVA-specific IgG total **(A-C)** and IgG1 **(D-F)** antibody titers measured in BALB/c mice on day 21 **(A and D)**, day 42 **(B and E)** and day 63 **(C and F)**. Bars represent mean ± SEM, n = 8. *p < 0.05, **p < 0.01. OVA, ovalbumin; HA, hyaluronan.

3.2 Analysis of CD4$^+$ T-cell activation *in vitro*

To determine whether the presence of different HA-MW, with or without OVA, affect cellular responses, OT-II T-cell (OVA-specific CD4$^+$ cells) activation studies were performed *in vitro*. As expected, addition of OVA induces OT-II proliferation, which is enhanced in the presence of LPS (Figure 2). The co-exposure of cells to OVA and HA however, regardless of the molecular weight, did not increase OT-II proliferation compared to OVA alone. In line with the antibody responses, this suggests that none of the tested HA polymer provided a measurable adjuvant effect.

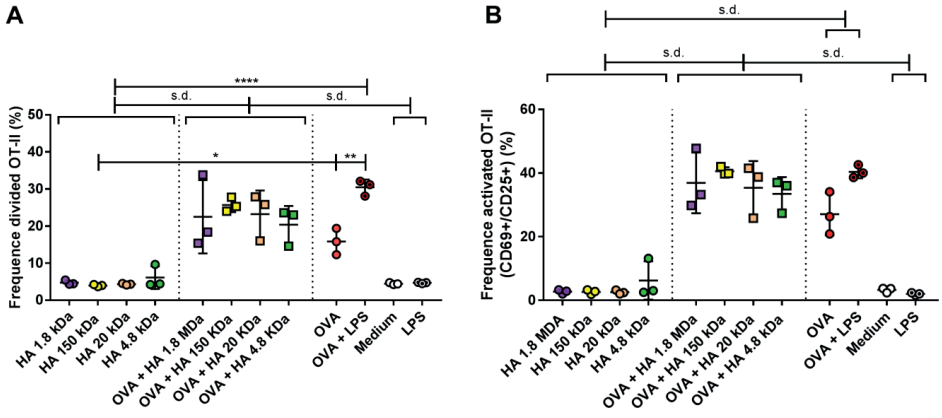

Figure 2. OT-II activation *in vitro*. **(A)** percentage of dividing cells, **(B)** percentage of $CD69^+/CD25^+$ cells. Bars represent mean ± SEM, n = 3. *p < 0.05, **p < 0.01. OVA, ovalbumin; HA, hyaluronan; LPS, lipopolysaccharide; s.d., significantly different.

3.3 Dissolving microneedle fabrication

The immunological analysis of the various HA polymers, suggests a preference for small MW polymer, as the high MW polymer show reduced antibody titers. Next we determined whether the MW of HA affected the fabrication of dissolving microneedles and their dissolution in the skin. Fabrication of dissolving microneedles was possible for the HA-MWs 150 kDa, 20 kDa and 4.8 kDa. The 10% (w/v) concentration of MW 1.8 MDa HA led to gel formation preventing the fabrication of microneedles. For the HA-MW 4.8 kDa, the fabrication of dissolving microneedles with a final step of drying at 37°C, as performed for the 150 kDa and 20 kDa HA, led to ruptures on the microneedle arrays surface (data not shown). Thus, the drying was performed at room temperature, resulting in intact microneedle arrays.

3.4 Penetration and dissolution of microneedles in *ex vivo* human skin

In order to assess whether the molecular weight of HA had an effect on the capability of microneedles to pierce and dissolve into the skin, first their ability to pierce *ex vivo* human skin was tested. Bright field analysis showed sharp microneedles regardless of the HA-MW (Figure 3A).The penetration efficiency of microneedles into the skin was not affected by the molecular weight of the HA. The 150 kDa microneedles showed a penetration efficiency of 96 ± 7%; 20 kDa and 4.8 kDa HA microneedles showed a penetration efficiency of 98 ± 4%, (mean ± SD, n=3).

Dissolution studies showed a gradual dissolution in time irrespective of the HA-MW (Figure 3A). However, while 20 kDa and 4.8 kDa HA dMNs completely dissolved within 20 minutes application in the skin (97 ± 2% and 100 ± 0% dissolved volumes respectively), the 150 kDa HA dMNs reached only 80% dissolved volume after the same application time (Figure 3A).

No differences in dissolved volumes between 20 kDa and 4.8 kDa HA microneedles at each application time were observed (Figure 3B), however the dissolved volume of the 150 kDa HA microneedles was significantly reduced at each time point compared to the other HA-MW microneedles. This resulted in a complete dissolution of the 20 kDa and 4.8 kDa HA microneedles after 10 minutes application, while the 150 kDa HA microneedles took 20 minutes to almost completely dissolve.

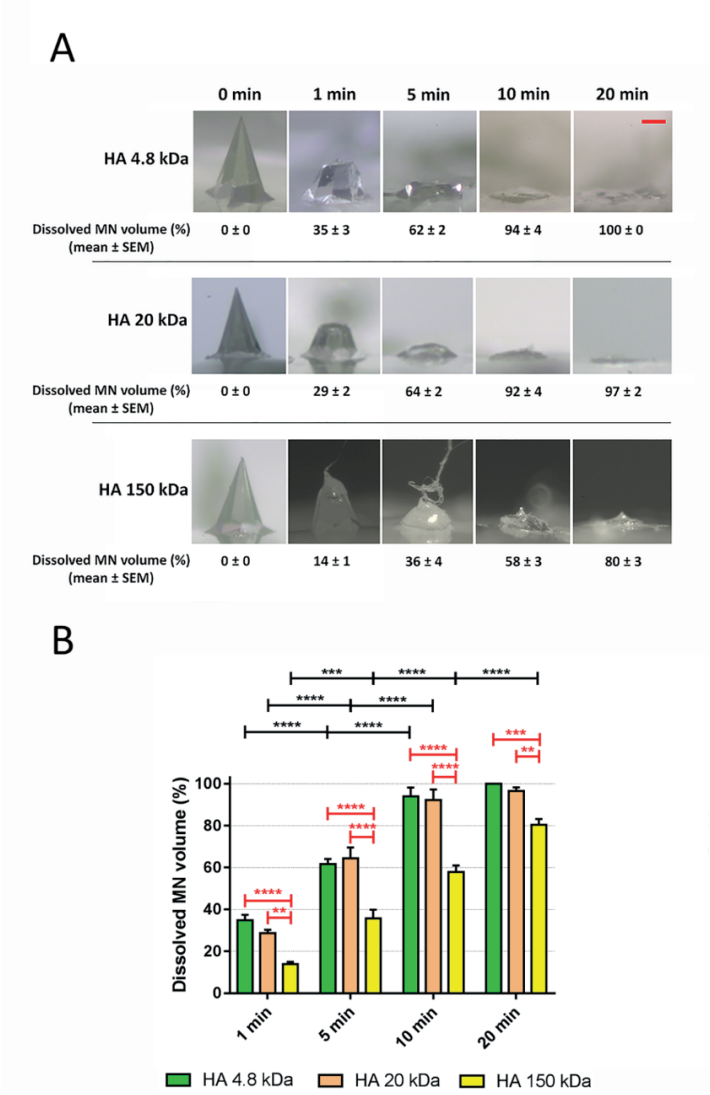

Figure 3. dMN dissolution in *ex vivo* human skin. **(A)** Representative bright field images (5x) of 10% (w/v) HA 4.8 kDa, 20 kDa and 150 kDa microneedle before application on the skin (0 min) and after 1, 5, 10 and 20 min dissolution in *ex vivo* human skin. Dissolved volumes are reported as mean ± SEM (n = 7). Scale bar 100 µm. **(B)** Effect of time (1, 5, 10 and 20 min) on dissolution per each HA-MW dMN type (statistics in black) and effect of HA-MWs on dissolution of dMNs at different time points (red statistics) are shown. Significance (**p<0.01, ***p<0.001 and ****p < 0.0001) was determined by a two-way ANOVA with a Tukey's post-test (n = 7). All data are presented as mean ± SEM. HA, hyaluronan.

4. DISCUSSION

When choosing the HA polymer for the fabrication of dMNs, it is relevant to investigate potential immune modulating effects besides effects related to the dMN manufacturing and physicochemical characteristics of dMNs such as capability to pierce the skin and dissolve quickly.

Although LMW-HA can have inflammatory properties in contrast to HMW-HA [19, 20, 22, 36, 37], to our knowledge, the role of HA-MW on the antibody response has not been reported yet. To this end, in the present study HA ranging from 4.8 kDa to 1.8 MDa mixed with OVA was injected intradermally in mice to assess the antibody response evoked. We did not observe an increase in antibody titers by adjuvanting with LMW-HA; however we did observe that HMW-HA (1.8 MDa) reduced the antibody level after the second boost compared to OVA only and LMW-HA 4.8 kDa HA mixed with OVA. This may be explained by reports that HMW-HA exerts an anti-inflammatory role reducing the side effects of vaccines [38, 39] and displays immunosuppressive properties [40-42]. To this end, it has been reported that HMW-HA up-regulates the transcription factor FOXP3 on regulatory T-cells (Treg) (e.g. $CD4^+$ $CD25^+$) [42] involved in the regulatory mechanism of autoantibody production [43] and likely antibody production. Although we did not investigate Treg activation in this study, they provide a potential mechanism regarding the lack of immunogenicity of HMW-HA.

The role of what in literature is defined as LMW-HA has been extensively investigated suggesting a pro-inflammatory effect *in vitro*: 4-6 oligosaccharides HA induced cytokine synthesis in dendritic cells [19, 20]; HA < 250 kDa induced inflammatory cytokines levels [36, 44-48]; HA ≤ 800 kDa led to activation of macrophages [37]. In this study, the effect of HA-MW was examined on the activation of $CD4^+$ T-cells. Although this is an *in vitro* system, it has shown to be predictive in the sense that formulations that induce strong *in vitro* response of OT-II cells also outperformed other formulations *in vivo* [49, 50]. Conversely to what has been reported in literature, changes in HA-MW did not influence the proliferation and activation of $CD4^+$ T-cells *in vitro*. Considerations justifying the referred controversial effects of HA preparations may be related to i) MW of HA that is not always measured accurately or is not homogeneous in the same HA population, for this reason an effect may be attributed to a minor population, ii) the presence of minor contaminants even in highly purified HA and iii) the conformational diversity of HA highly dependent on pH, temperature, salt concentration and specific cations [48]. Furthermore, the effects of HA-MW seems to be cell-specific and depending on the HA medium concentration [26, 48]. However, in literature there is not an optimal HA concentration reported and often the same concentration of different HA-MWs may have opposite effects on $CD4^+$ cellular response [42]. This lack of data should be addressed in future investigations, i.e. i) HAs in a wide range of concentrations with a dose/response on specific cell types and ii) cytokines produced by DCs

and $CD4^+$ T-cells after exposure to the HA formulations, to obtain additional information on the regulatory effect of HA.

Due to the absence of intrinsic adjuvant properties of HA, regardless of the molecular weight, all the HA-MWs were tested for potential effects on the manufacturing of dMNs and their capability to penetrate the skin and quickly dissolve. As reported in literature, a factor influencing the dMN dissolution time in the skin is the HA concentration [10, 51]. However, to our knowledge, the role of the HA-MW on the dMN dissolution in the skin is reported in the present study for the first time highlighting the novelty of this study. HA is being used in experimental drug delivery systems. The lack of immune activation of HA, regardless MW may be used to taylor drug release kinetics. However, although we did not show immunological effects, using low MW HA, may introduce safety concerns, since low MW fragments (oligomers) are associated with inflammatory responses [52].

Difficulties or impossibility in dMN fabrication when choosing too low (4.8 kDa) or high (1.8 MDa) HA-MWs, respectively, identified an optimal HA-MW in the middle range (20 kDa and 150 kDa). The 4.8 kDa HA could only be formulated into dMN by drying at room temperature to avoid ruptures of the dMN arrays. Although drying at low temperature (room temperature) can preserve the antigen stability, it may lead to long processing time not compatible with scalability in fabrication and to a higher residual moisture content in dMN than drying at high temperature, potentially resulting in decrease in antigen stability. The HA-MW 1.8 MDa formed a gel, due to the high viscosity, preventing further processing into dMNs. Furthermore, increase in HA-MW led to prolonged application time for a complete dMN dissolution into the skin.

Based on the result described above, the 20 kDa HA should be preferred to the 4.8 kDa and 150 kDa HA for the fabrication of dMNs.

5. CONCLUSIONS

The present study underlines the importance of defining a specific HA-MW for the fabrication of dMNs based on the investigation and assessment of the effects of the HA-MW on the immune response and on the physicochemical characteristics of dMNs such as capability to pierce the skin and dissolve quickly.

We consider, among the HA-MWs investigated, the medium-low HA-MW of 20 kDa the optimal MW as it results in robust dMNs characterized by a fast dissolving process in the skin and has no effect on the immunogenicity of the antigen.

REFERENCES

1. S. Hirobe, H. Azukizawa, T. Hanafusa, K. Matsuo, Y.S. Quan, F. Kamiyama, I. Katayama, N. Okada, S. Nakagawa, Clinical study and stability assessment of a novel transcutaneous influenza vaccination using a dissolving microneedle patch, Biomaterials, 57 (2015) 50-58.
2. J. Arya, S. Henry, H. Kalluri, D.V. McAllister, W.P. Pewin, M.R. Prausnitz, Tolerability, usability and acceptability of dissolving microneedle patch administration in human subjects, Biomaterials, 128 (2017) 1-7.
3. M. Leone, J. Monkare, J.A. Bouwstra, G. Kersten, Dissolving Microneedle Patches for Dermal Vaccination, Pharm Res, 34 (2017) 2223-2240.
4. K. van der Maaden, W. Jiskoot, J. Bouwstra, Microneedle technologies for (trans)dermal drug and vaccine delivery, J Control Release, 161 (2012) 645-655.
5. E. Larraneta, R.E.M. Lutton, A.D. Woolfson, R.F. Donnelly, Microneedle arrays as transdermal and intradermal drug delivery systems: Materials science, manufacture and commercial development, Mat Sci Eng R, 104 (2016) 1-32.
6. E. Larraneta, M.T. McCrudden, A.J. Courtenay, R.F. Donnelly, Microneedles: A New Frontier in Nanomedicine Delivery, Pharm Res, 33 (2016) 1055-1073.
7. T.M. Tuan-Mahmood, M.T. McCrudden, B.M. Torrisi, E. McAlister, M.J. Garland, T.R. Singh, R.F. Donnelly, Microneedles for intradermal and transdermal drug delivery, Eur J Pharm Sci, 50 (2013) 623-637.
8. K. van der Maaden, R. Luttge, P.J. Vos, J. Bouwstra, G. Kersten, I. Ploemen, Microneedle-based drug and vaccine delivery via nanoporous microneedle arrays, Drug Deliv Transl Re, 5 (2015) 397-406.
9. S. Hirobe, H. Azukizawa, K. Matsuo, Y. Zhai, Y.S. Quan, F. Kamiyama, H. Suzuki, I. Katayama, N. Okada, S. Nakagawa, Development and Clinical Study of a Self-Dissolving Microneedle Patch for Transcutaneous Immunization Device, Pharm Res-Dordr, 30 (2013) 2664-2674.
10. M. Leone, M.I. Priester, S. Romeijn, M.R. Nejadnik, J. Monkare, C. O'Mahony, W. Jiskoot, G. Kersten, J.A. Bouwstra, Hyaluronan-based dissolving microneedles with high antigen content for intradermal vaccination: Formulation, physicochemical characterization and immunogenicity assessment, Eur J Pharm Biopharm, 134 (2019) 49-59.
11. K. Matsuo, S. Hirobe, Y. Yokota, Y. Ayabe, M. Seto, Y.S. Quan, F. Kamiyama, T. Tougan, T. Horii, Y. Mukai, N. Okada, S. Nakagawa, Transcutaneous immunization using a dissolving microneedle array protects against tetanus, diphtheria, malaria, and influenza (vol 160, pg 495, 2012), J Control Release, 184 (2014) 18-19.
12. K. Matsuo, Y. Yokota, Y. Zhai, Y.S. Quan, F. Kamiyama, Y. Mukai, N. Okada, S. Nakagawa, A low-invasive and effective transcutaneous immunization system using a novel dissolving microneedle array for soluble and particulate antigens (vol 161, pg 10, 2012), J Control Release, 184 (2014) 9-9.
13. Z. Zhu, X. Ye, Z. Ku, Q. Liu, C. Shen, H. Luo, H. Luan, C. Zhang, S. Tian, C. Lim, Z. Huang, H. Wang, Transcutaneous immunization via rapidly dissolvable microneedles protects against hand-foot-and-mouth disease caused by enterovirus 71, J Control Release, 243 (2016) 291-302.
14. E.J. Oh, K. Park, K.S. Kim, J. Kim, J.A. Yang, J.H. Kong, M.Y. Lee, A.S. Hoffman, S.K. Hahn, Target specific and long-acting delivery of protein, peptide, and nucleotide therapeutics using hyaluronic acid derivatives, J Control Release, 141 (2010) 2-12.
15. Y. Ito, S. Kashiwara, K. Fukushima, K. Takada, Two-layered dissolving microneedles for percutaneous delivery of sumatriptan in rats, Drug Dev Ind Pharm, 37 (2011) 1387-1393.
16. S. Liu, M.N. Jin, Y.S. Quan, F. Kamiyama, H. Katsumi, T. Sakane, A. Yamamoto, The development and characteristics of novel microneedle arrays fabricated from hyaluronic acid, and their application in the transdermal delivery of insulin, J Control Release, 161 (2012) 933-941.

17. S. Liu, D. Wu, Y.S. Quan, F. Kamiyama, K. Kusamori, H. Katsumi, T. Sakane, A. Yamamoto, Improvement of Transdermal Delivery of Exendin-4 Using Novel Tip-Loaded Microneedle Arrays Fabricated from Hyaluronic Acid, Mol Pharm, 13 (2016) 272-279.
18. P.W. Noble, Hyaluronan and its catabolic products in tissue injury and repair, Matrix Biol, 21 (2002) 25-29.
19. C.C. Termeer, J. Hennies, U. Voith, T. Ahrens, J.M. Weiss, P. Prehm, J.C. Simon, Oligosaccharides of hyaluronan are potent activators of dendritic cells, J Immunol, 165 (2000) 1863-1870.
20. C. Termeer, F. Benedix, J. Sleeman, C. Fieber, U. Voith, T. Ahrens, K. Miyake, M. Freudenberg, C. Galanos, J.C. Simon, Oligosaccharides of Hyaluronan activate dendritic cells via toll-like receptor 4, J Exp Med, 195 (2002) 99-111.
21. U.M. Agren, R.H. Tammi, M.I. Tammi, Reactive oxygen species contribute to epidermal hyaluronan catabolism in human skin organ culture, Free Radic Biol Med, 23 (1997) 996-1001.
22. P.W. Noble, C.M. McKee, M. Cowman, H.S. Shin, Hyaluronan fragments activate an NF-kappa B/I-kappa B alpha autoregulatory loop in murine macrophages, J Exp Med, 183 (1996) 2373-2378.
23. J. Muto, Y. Morioka, K. Yamasaki, M. Kim, A. Garcia, A.F. Carlin, A. Varki, R.L. Gallo, Hyaluronan digestion controls DC migration from the skin, J Clin Invest, 124 (2014) 1309-1319.
24. D.N. Hart, Dendritic cells: unique leukocyte populations which control the primary immune response, Blood, 90 (1997) 3245-3287.
25. J. Lesley, N. Howes, A. Perschl, R. Hyman, Hyaluronan-Binding Function of Cd44 Is Transiently Activated on T-Cells during an in-Vivo Immune-Response, J Exp Med, 180 (1994) 383-387.
26. S. Mizrahy, S.R. Raz, M. Hasgaard, H. Liu, N. Soffer-Tsur, K. Cohen, R. Dvash, D. Landsman-Milo, M.G. Bremer, S.M. Moghimi, D. Peer, Hyaluronan-coated nanoparticles: the influence of the molecular weight on CD44-hyaluronan interactions and on the immune response, J Control Release, 156 (2011) 231-238.
27. D.H. Jiang, J.R. Liang, P.W. Noble, Hyaluronan as an Immune Regulator in Human Diseases, Physiol Rev, 91 (2011) 221-264.
28. C.S. Termeer, J. P.; Simon, J. C., Hyaluronan – magic glue for the regulation of the immune response?, TRENDS in Immunology, 24 (2003) 112-114.
29. H. Kono, K.L. Rock, How dying cells alert the immune system to danger, Nature Reviews Immunology, 8 (2008) 279-289.
30. M. Leone, M.I. Priester, S. Romeijn, M.R. Nejadnik, J. Monkare, C. O'Mahony, W. Jiskoot, G. Kersten, J.A. Bouwstra, Hyaluronan-based dissolving microneedles with high antigen content for intradermal vaccination: Formulation, physicochemical characterization and immunogenicity assessment, Eur J Pharm Biopharm, 134 (2019) 49-59.
31. N. Wilke, M.L. Reed, A. Morrissey, The evolution from convex corner undercut towards microneedle formation: theory and experimental verification, J Micromech Microeng, 16 (2006) 808-814.
32. P. Schipper, K. van der Maaden, S. Romeijn, C. Oomens, G. Kersten, W. Jiskoot, J. Bouwstra, Determination of Depth-Dependent Intradermal Immunogenicity of Adjuvanted Inactivated Polio Vaccine Delivered by Microinjections via Hollow Microneedles, Pharm Res, 33 (2016) 2269-2279.
33. K. van der Maaden, S.J. Trietsch, H. Kraan, E.M. Varypataki, S. Romeijn, R. Zwier, H.J. van der Linden, G. Kersten, T. Hankemeier, W. Jiskoot, J. Bouwstra, Novel hollow microneedle technology for depth-controlled microinjection-mediated dermal vaccination: a study with polio vaccine in rats, Pharm Res, 31 (2014) 1846-1854.
34. M. Leone, B.H. van Oorschot, M.R. Nejadnik, A. Bocchino, M. Rosato, G. Kersten, C. O'Mahony, J. Bouwstra, K. van der Maaden, Universal Applicator for Digitally-Controlled Pressing Force and Impact Velocity Insertion of Microneedles into Skin, Pharmaceutics, 10 (2018).

35. K. van der Maaden, E. Sekerdag, W. Jiskoot, J. Bouwstra, Impact-insertion applicator improves reliability of skin penetration by solid microneedle arrays, Aaps J, 16 (2014) 681-684.
36. A. D'Agostino, A. Stellavato, L. Corsuto, P. Diana, R. Filosa, A. La Gatta, M. De Rosa, C. Schiraldi, Is molecular size a discriminating factor in hyaluronan interaction with human cells?, Carbohyd Polym, 157 (2017) 21-30.
37. J.E. Rayahin, J.S. Buhrman, Y. Zhang, T.J. Koh, R.A. Gemeinhart, High and Low Molecular Weight Hyaluronic Acid Differentially Influence Macrophage Activation, Acs Biomater Sci Eng, 1 (2015) 481-493.
38. L. Topazio, R. Miano, V. Maurelli, G. Gaziev, M. Gacci, V. Iacovelli, E. Finazzi-Agro, Could Hyaluronic acid (HA) reduce Bacillus Calmette-Guerin (BCG) local side effects? Results of a pilot study, Bmc Urol, 14 (2014).
39. F. Zamboni, S. Vieira, R.L. Reis, J.M. Oliveira, M.N. Collins, The potential of hyaluronic acid in immunoprotection and immunomodulation: Chemistry, processing and function, Prog Mater Sci, 97 (2018) 97-122.
40. M. Litwiniuk, A. Krejner, T. Grzela, Hyaluronic Acid in Inflammation and Tissue Regeneration, Wounds, 28 (2016) 78-88.
41. T. Chanmee, P. Ontong, N. Itano, Hyaluronan: A modulator of the tumor microenvironment, Cancer Lett, 375 (2016) 20-30.
42. P.L. Bollyky, J.D. Lord, S.A. Masewicz, S.P. Evanko, J.H. Buckner, T.N. Wight, G.T. Nepom, Cutting edge: high molecular weight hyaluronan promotes the suppressive effects of CD4+CD25+ regulatory T cells, J Immunol, 179 (2007) 744-747.
43. W.T. Hsu, J.L. Suen, B.L. Chiang, The role of CD4(+)CD25(+) T cells in autoantibody production in murine lupus, Clin Exp Immunol, 145 (2006) 513-519.
44. J. Hodge-Dufour, P.W. Noble, M.R. Horton, C. Bao, M. Wysoka, M.D. Burdick, R.M. Strieter, G. Trinchieri, E. Pure, Induction of IL-12 and chemokines by hyaluronan requires adhesion-dependent priming of resident but not elicited macrophages, J Immunol, 159 (1997) 2492-2500.
45. M.R. Horton, M.D. Burdick, R.M. Strieter, G. Bao, P.W. Noble, Regulation of hyaluronan-induced chemokine gene expression by IL-10 and IFN-gamma in mouse macrophages, J Immunol, 160 (1998) 3023-3030.
46. C.M. McKee, M.B. Penno, M. Cowman, M.D. Burdick, R.M. Strieter, C. Bao, P.W. Noble, Hyaluronan (HA) fragments induce chemokine gene expression in alveolar macrophages. The role of HA size and CD44, J Clin Invest, 98 (1996) 2403-2413.
47. P.W. Noble, F.R. Lake, P.M. Henson, D.W. Riches, Hyaluronate activation of CD44 induces insulin-like growth factor-1 expression by a tumor necrosis factor-alpha-dependent mechanism in murine macrophages, J Clin Invest, 91 (1993) 2368-2377.
48. R. Stern, A.A. Asari, K.N. Sugahara, Hyaluronan fragments: an information-rich system, Eur J Cell Biol, 85 (2006) 699-715.
49. C. Keijzer, B. Slutter, R. van der Zee, W. Jiskoot, W. van Eden, F. Broere, PLGA, PLGA-TMC and TMC-TPP nanoparticles differentially modulate the outcome of nasal vaccination by inducing tolerance or enhancing humoral immunity, Plos One, 6 (2011) e26684.
50. N. Benne, J. van Duijn, F. Lozano Vigario, R.J.T. Leboux, P. van Veelen, J. Kuiper, W. Jiskoot, B. Slutter, Anionic 1,2-distearoyl-sn-glycero-3-phosphoglycerol (DSPG) liposomes induce antigen-specific regulatory T cells and prevent atherosclerosis in mice, J Control Release, 291 (2018) 135-146.
51. J. Monkare, M. Reza Nejadnik, K. Baccouche, S. Romeijn, W. Jiskoot, J.A. Bouwstra, IgG-loaded hyaluronan-based dissolving microneedles for intradermal protein delivery, J Control Release, 218 (2015) 53-62.
52. A. Passi, D. Vigetti, Hyaluronan as tunable drug delivery system, Adv Drug Deliver Rev, 146 (2019) 83-96.

SUPPLEMENTARY MATERIAL

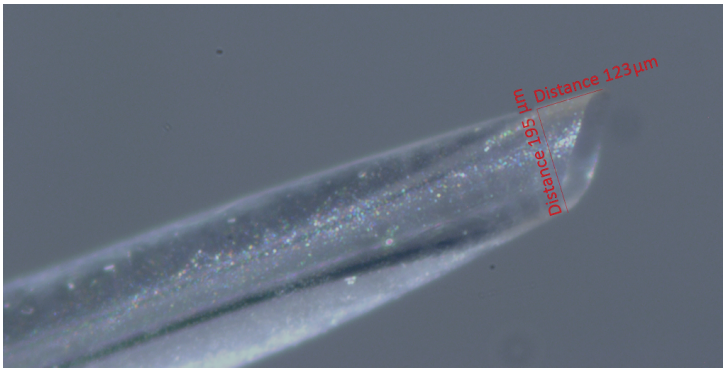

Supplementary Figure S1. Representative bright field microscope image of a hMN. The diameter of approximately 195 µm and the microneedle tip of approximately 120 µm piercing in the skin are reported on the figure.

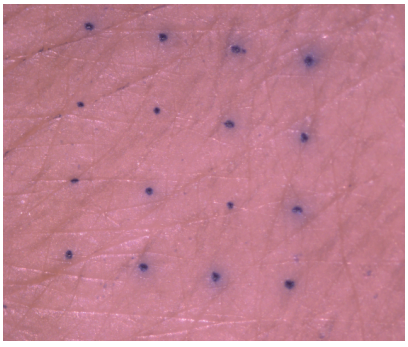

Supplementary Figure S2. Representative bright field microscope image of pierced *ex vivo* human skin after staining with trypan blue and *stratum corneum* stripping by tape.